Frequency of the transition spectral line of an electron in quantum rods*

Wang Guiwen(王贵文)[1] and Xiao Jinglin(肖景林)[2,†]

(1 College of Physics and Electronic Information, Inner Mongolia Hulunbei'er College, Hulunbei'er 021008, China)
(2 College of Physics and Electronic Information, Inner Mongolia National University, Tongliao 028043, China)

Abstract: The Hamiltonian of a quantum rod with an ellipsoidal boundary is given after a coordinate transformation which changes the ellipsoidal boundary into a spherical one. We then study the first internal excited state energy, the excitation energy and the frequency of the transition spectral line between the first internal excited state and the ground state of the strong-coupling polaron in a quantum rod. The effects of the electron–phonon coupling strength, the aspect ratio of the ellipsoid, the transverse radius of quantum rods and the transverse and longitudinal effective confinement length are taken into consideration by using a linear combination operator and the unitary transformation methods. It is found that the first internal excited state energy, the excitation energy and the frequency of the transition spectral line are increasing functions of the electron–phonon coupling strength, whereas they are decreasing ones of the transverse radius of quantum rods and the aspect ratio. The first internal excited state energy, the excitation energy and the frequency of the transition spectral line increase with decreasing transverse and longitudinal effective confinement length.

Key words: quantum rods; polaron; linear combination operator; aspect ratio
DOI: 10.1088/1674-4926/31/9/092002 **PACC:** 7138; 7320D

1. Introduction

Semiconductor quantum rods or nanorods are colloidal quantum dots with strong radial confinement and variable length[1, 2]. Ever since the shape controlled colloidal quantum rod was realized in experiments by modifying the synthesis[2, 3], it has become a major subject of interest because of the freedom it offers in material tailoring and its much wider application ranges, such as biological labeling[4, 5] and optoelectronic devices[6]. Its novel electronic structures, optical properties, and linearly polarized emission have become a hot field of investigation in quantum functional devices. Many investigators have studied the properties of quantum rods in many aspects by a variety of theoretical and experimental methods[7−14]. Katz *et al.*[15] used the combined optical and tunneling spectroscopy method to investigate the electronic level structure of CdSe quantum rods, and showed its dependence on rod length and diameter. Li and Xia[16] investigated the electronic structure and optical properties of a wurtzite quantum rod in the framework of the effective-mass envelope-function theory. The high energy exciton states of large CdSe quantum rods, including spin-orbital coupling and screened electron-hole Coulomb interaction, were calculated by Li *et al.*[17], using the plane-wave pseudopotential method. Zhang *et al.*[18] introduced a theoretical model in the framework of the eight-band effective-mass approximation in the presence of an external homogeneous magnetic field to investigate the electronic structure, optical properties and electron g factors of GaAs quantum rods. The interaction between electron–electron and electron–hole pairs in semiconductor nanorods embedded in dielectric media was investigated by Climente *et al.*[19] using a configuration-interaction method . The experimental data were compared by Talaat *et al.*[20] to that calculated using two theoretical models, i.e., the effective mass approximation and the semi-empirical pseudopotential method. The theoretical values for the energy band gap at varying radii are in agreement with the experimental results within 0.08 eV. Using the linear-combination operator and unitary transformation methods, the properties of the weak-coupling polaron in a quantum rod have been studied by us[21]. The properties of the excited state of a polaron in quantum rods, however, have not been studied so far by employing the linear-combination operator method.

In the present paper, we investigate the effects of the ellipsoid aspect ratio, the electron–phonon coupling strength, the transverse radius of quantum rods and the transverse and longitudinal effective confinement length on the first internal excited state energy, the excitation energy and the frequency of the transition spectral line of a strongly-coupled polaron in a quantum rod by using the linear-combination operator and unitary transformation methods. It should be noted that as long as the boundary potential of the quantum rod is transformed from the ellipsoidal form into a spherical one, we can conveniently use the linear-combination operator in the framework of the effective-mass approximation to calculate the relevant physical quantities, and do not have to use the boundary condition of the electron functions.

2. Theoretical model

The electron under consideration is moving in a polar crystal quantum rod with three-dimensional anisotropic harmonic potential, and is interacting with bulk LO phonons. The Hamiltonian of the electron–phonon interaction system in the quantum rods can be written as Eq. (1).

* Project supported by the National Natural Science Foundation of China (No. 10747002).
† Corresponding author. Email: xiaojlin@126.com
Received 9 January 2010, revised manuscript received 21 March 2010

$$H=\frac{p_{\parallel}^{2}}{2m}+\frac{p_{z}^{2}}{2m}+\sum_{\boldsymbol{q}}\hbar\omega_{\mathrm{LO}}a_{\boldsymbol{q}}^{+}a_{\boldsymbol{q}}+\frac{1}{2}m\omega_{\parallel}^{2}\rho^{2}+\frac{1}{2}m\omega_{z}^{2}z^{2}+\sum_{\boldsymbol{q}}\left[V_{q}a_{\boldsymbol{q}}\exp\left(i\boldsymbol{q}\cdot\boldsymbol{r}\right)+h.c\right],\tag{1}$$

where m is the band mass, and $\omega_{\parallel}$ and ω_z are the measure of the transverse and longitudinal confinement strengths of the three-dimensional anisotropic harmonic potential in the xy plane and the z direction, respectively. $a_{\boldsymbol{q}}^{+}\left(a_{\boldsymbol{q}}\right)$ denotes the creation (annihilation) operator of the bulk LO phonons with wave vector $\boldsymbol{q}(q_{\perp},\boldsymbol{q}_{\parallel})$, $\boldsymbol{r}=(\rho,z)$ is the position vector of the electron, and

$$V_{\boldsymbol{q}}=i\left(\frac{\hbar\omega_{\mathrm{LO}}}{q}\right)\left(\frac{\hbar}{2m\omega_{\mathrm{LO}}}\right)^{1/4}\left(\frac{4\pi\alpha}{v}\right)^{1/2},\quad \alpha=\left(\frac{e^{2}}{2\hbar\omega_{\mathrm{LO}}}\right)\left(\frac{2m\omega_{\mathrm{LO}}}{\hbar}\right)^{1/2}\left(\frac{1}{\varepsilon_{\infty}}-\frac{1}{\varepsilon_{0}}\right).\tag{2}$$

For quantum rods, the boundary condition is different from that of spherical quantum dots. In order to transform our boundary condition into a spherical one, which has a better symmetrical characteristic, we introduce a coordinate transformation[16]. The transformation is $x'=x$, $y'=y$, $z'=z/e'$, where e' is the aspect ratio of the ellipsoid, $(x,\ y,\ z)$ is the actual coordinate, and $(x',\ y',\ z')$ is the transformed one. The electron–phonon system Hamiltonian in the new coordinate is changed as follows:

$$H=\frac{p_{\parallel'}^{2}}{2m}+\frac{e'^{2}p_{z'}^{2}}{2m}+\sum_{\boldsymbol{q}}\hbar\omega_{\mathrm{LO}}a_{\boldsymbol{q}}^{+}a_{\boldsymbol{q}}+\frac{1}{2}m\omega_{\parallel'}^{2}\rho'^{2}+\frac{1}{2e'^{2}}m\omega_{z'}^{2}z'^{2}+\sum_{\boldsymbol{q}}\left[V_{q}a_{\boldsymbol{q}}\exp\left(i\boldsymbol{q}_{\parallel'}\cdot\boldsymbol{\rho}'+iq_{z'}z'e'\right)+h.c\right].\tag{3}$$

We introduce a linear combination operator:

$$p_{\mathrm{j}}=\left[\frac{m\hbar\lambda}{2}\right]^{1/2}\left(b_{\mathrm{j}}+b_{\mathrm{j}}^{+}\right),\quad r_{\mathrm{j}}=i\left[\frac{\hbar}{2m\lambda}\right]^{1/2}\left(b_{\mathrm{j}}-b_{\mathrm{j}}^{+}\right),\quad j=x,y,z,\tag{4}$$

where λ is the variational parameters**.** Inserting Eq. (4) into Eq. (3), we then carry out the unitary transformation to Eq. (3):

$$U=\exp\left[\sum_{\boldsymbol{q}}(a_{\boldsymbol{q}}^{+}f_{\mathrm{q}}-a_{\boldsymbol{q}}f_{\mathrm{q}}^{*})\right],\tag{5}$$

where $f_{\mathrm{q}}(f_{\mathrm{q}}^{*})$ is the variational function. The ground- and first internal excited-state wave function of the system is chosen as

$$|\Psi_{0}\rangle=|0\rangle_{a}|0\rangle_{b},\tag{6}$$

$$|\psi_{1}\rangle=|0\rangle_{a}|1\rangle_{b},\quad |1\rangle_{b}=b^{+}|0\rangle_{b},\tag{7}$$

where $|0\rangle_{b}$ is the vacuum state of the b operator, and $|0\rangle_{a}$ is the unperturbed zero-phonon state. We now obtain

$$F_{0}\left(\lambda,f_{\mathrm{q}}\right)=\langle\psi_{0}|\,U^{-1}HU\,|\psi_{0}\rangle.\tag{8}$$

Performing the variation of $F_0(\lambda,\ f_{\mathrm{q}})$ with respect to λ and f_{q}, we obtain the ground state energy E_0 of the strong-coupling polaron.

The expectation value of Eq. (3) with respect to $|\psi_1\rangle$ can be expressed as

$$F_{1}\left(\lambda,f_{q}\right)=\langle\psi_{1}|\,U^{-1}HU\,|\psi_{1}\rangle.\tag{9}$$

If we choose the usual polaron unit ($\hbar=2m=\omega_{\mathrm{LO}}=1$), using the variational method, the first internal excited state energy of the strong-coupling polaron in a quantum rod can be written as

$$E_{1}=\lambda_{0}+\frac{3e'^{2}}{4}\lambda_{0}+\frac{4}{\lambda_{0}l_{\mathrm{p}}^{4}}+\frac{3}{\lambda_{0}l_{\mathrm{v}}^{4}e'^{2}}-\frac{2\alpha}{3\sqrt{\pi}}\sqrt{\lambda_{0}}A\left(e'\right),\tag{10}$$

$A(e')$ is written as

$$A(e')=\begin{cases}\dfrac{\arcsin\sqrt{1-e'^{2}}}{\sqrt{1-e'^{2}}}, & e'<1,\\[2ex] 1, & e'=1,\\[2ex] \dfrac{1}{2\sqrt{e'^{2}-1}}\ln\dfrac{e'+\sqrt{e'^{2}-1}}{e'-\sqrt{e'^{2}-1}}, & e'>1,\end{cases}\tag{11}$$

where $l_{\mathrm{p}}=\sqrt{\hbar/m\omega_{\parallel'}}$, $l_{\mathrm{v}}=\sqrt{\hbar/m\omega_{z'}}$ are the transverse and longitudinal effective confinement lengths, respectively. If E_0 and E_1 denotes the energies of the ground- and first internal excited-state, respectively, then the excitation energy of the strong-coupling polaron in a quantum rod is given by

$$\Delta E=E_{1}-E_{0}=\frac{\lambda_{0}}{2}\left(1+e'^{2}\right)+\frac{2}{\lambda_{0}l_{p}^{4}}+\frac{2}{\lambda_{0}l_{v}^{4}e'^{2}}+\frac{2\alpha\sqrt{\lambda_{0}}}{3\sqrt{\pi}}A\left(e'\right).\tag{12}$$

The frequency of the transition spectral line between the first internal excited state and the ground state of the strong-coupling polaron in a quantum rod can be expressed as

$$\omega=\frac{E_{1}-E_{0}}{\hbar}=\frac{\lambda_{0}}{2}\left(1+e'^{2}\right)+\frac{2}{\lambda_{0}l_{\mathrm{p}}^{4}}+\frac{2}{\lambda_{0}l_{\mathrm{v}}^{4}e'^{2}}+\frac{\alpha\sqrt{\lambda_{0}}}{3\sqrt{\pi}}A\left(e'\right).\tag{13}$$

3. Numerical results and discussion

Now we perform numerical calculations to show the effect of the electron–phonon coupling strength α, the aspect ratio e' of the ellipsoid, the transverse radius R of quantum rods and

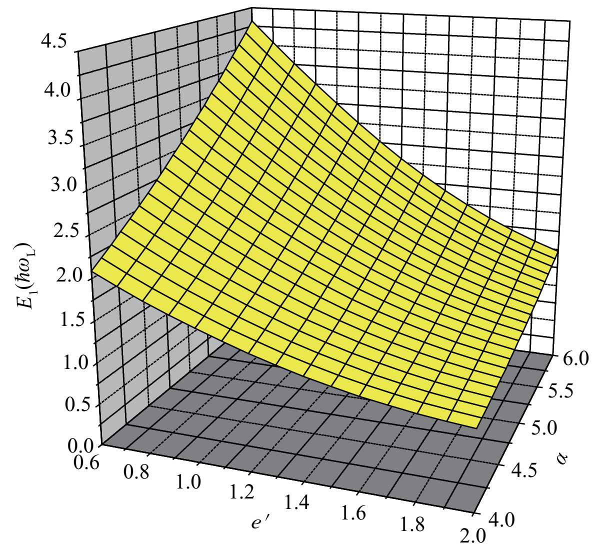

Fig. 1. Relational curves of the first internal excited state energy E_1 with the electron–phonon coupling strength α and the aspect ratio e' of the ellipsoid for fixed $l_p = 4$ and $l_v = 2$.

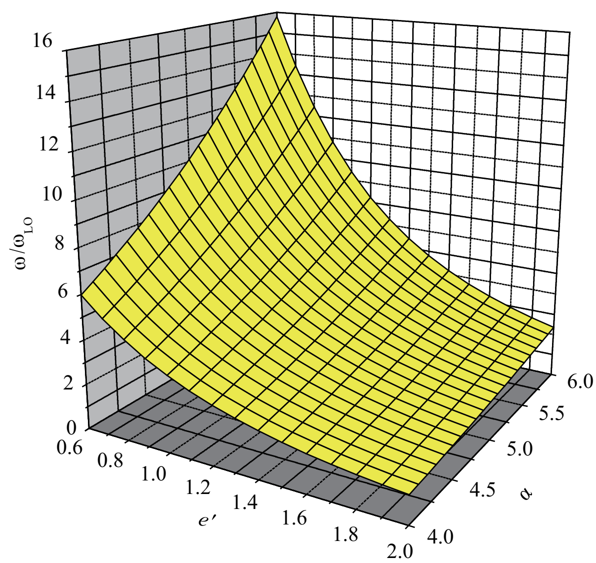

Fig. 2. Relational curves of the frequency ω of the transition spectral line with the electron–phonon coupling strength α and the aspect ratio e' of the ellipsoid for fixed $l_p = 4$ and $l_v = 2$.

the transverse and longitudinal effective confinement length l_p and l_v on the polaron's first internal excited state energy E_1, the excitation energy ΔE and the frequency ω of the transition spectral line between the first internal excited state and the ground state.

Figures 1 and 2 show the relationship between the first internal excited state energy E_1 and the frequency ω of the transition spectral line of the strong-coupled polaron in a quantum rod varying with the electron–phonon coupling strength α and the aspect ratio e' of the ellipsoid for fixed $l_p = 4$, $l_v = 2$, respectively. From the two figures we can see that they will increase with increasing electron–phonon coupling strength α. This is because the larger the electron–phonon coupling strength is, the stronger the electron–phonon interaction is.

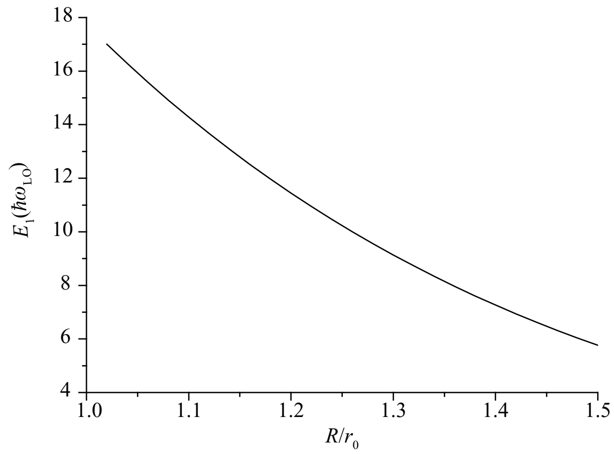

Fig. 3. Relational curves of the first internal excited state energy E_1 with the transverse radius R of quantum rods for fixed $l_p = 2, l_v = 3$, $L = 5.5$ and $\alpha = 4$.

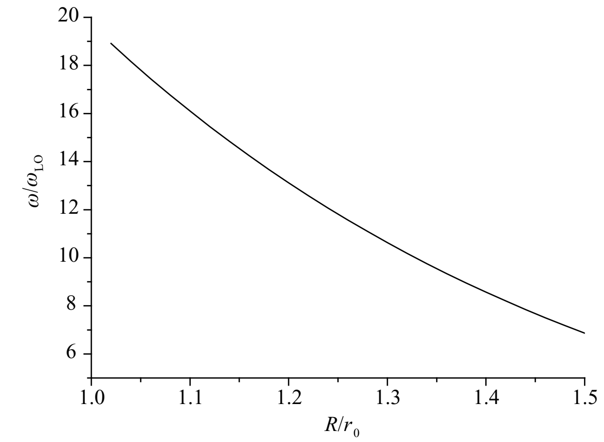

Fig. 4. Relational curves of the frequency ω of the transition spectral line with the transverse radius R of quantum rods for fixed $l_p = 2, l_v = 3$, $L = 5.5$ and $\alpha = 4$.

Therefore, it leads to the electron energy increment and makes the electrons interact with more phonons. As a result, the first internal excited state energy and the frequency of the transition spectral line of the strong-coupling polaron are all increased. From the two figures we can also see that the first internal excited state energy E_1 and the frequency ω of the transition spectral line are decreasing functions of the aspect ratio e'. These results are in agreement with those of Refs. [16, 17, 22]. For ellipsoidal quantum rods, we can define the aspect ratio of the ellipsoid as $e' = L/2R$, where L and R are the longitudinal length and the transverse radius of the rod, respectively. With the increase of e', that is, by increasing the longitudinal length L of the rod, the electron thermal motion energy and the interaction between the electrons and the phonons, which take the phonons as the medium, are reduced because of the larger motion space of the particles. As a result, the first internal excited state energy and the frequency of the transition spectral line of the polaron are all decreased with increasing e'. This result is similar to that of the quantum wire case, which was obtained in Ref. [23]. Conversely, with the decrease of the aspect ratio e', the electron thermal motion energy and the in-

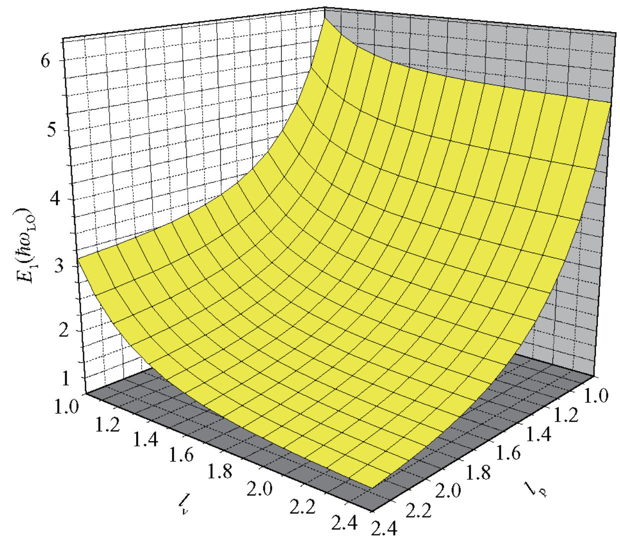

Fig. 5. Relational curves of the first internal excited state energy E_1 with the transverse and longitudinal effective confinement length l_p and l_v for fixed $a = 4.0, e' = 1.4$.

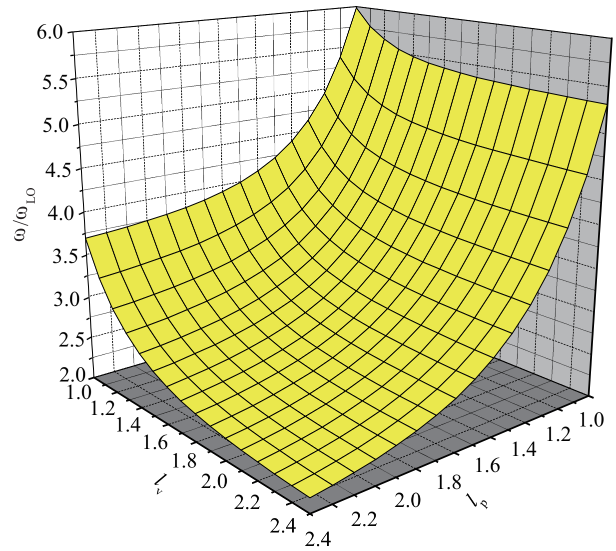

Fig. 6. Relational curves of the frequency ω of the transition spectral line with the transverse and longitudinal effective confinement length l_p and l_v for fixed $a = 4.0, e' = 1.4$.

teraction between the electrons and phonons are enhanced because of the smaller particle motion space. Correspondingly, the first internal excited state energy and the frequency of the transition spectral line are all increased, due to the interesting quantum size effects. This result is also similar to that of the quantum well case in Ref. [24].

Figures 3 and 4 show the relationship between the first internal excited state energy E_1 and the frequency ω of the transition spectral line as a function of the transverse radius R of quantum rods for $l_p = 2, l_v = 3$, $L = 5.5$, $\alpha = 4$ respectively. From the two figures we can see that they will decrease on increasing the transverse radius R of quantum rods. With the decrease of the transverse radius R, the thermal motion energy of the electrons and the interaction between an electron and the phonons, which take phonons as the medium, are enhanced because of the smaller range of particle motion. As a result of it, the first internal excited state energy and the frequency of the transition spectral line of the polaron are all increased. This result is in agreement with that of Ref. [15].

Figures 5 and 6 depict the first internal excited state energy E_1 and the frequency ω of the transition spectral line as functions of the transverse and longitudinal effective confinement length l_p and l_v for fixed $a = 4.0, e' = 1.4$, respectively. From the two figures we can see that they will increase with decreasing transverse and longitudinal effective confinement length l_p and l_v. From the expressions of $l_p = \sqrt{\hbar/m\omega_{\parallel'}}$ and $l_v = \sqrt{\hbar/m\omega_{z'}}$, we can see that the effective confinement length l_p and l_v are reciprocal with the square root of the confinement strength $\omega_{\parallel'}$ and $\omega_{z'}$, and then the first internal excited state energy and the frequency of the transition spectral line will increase with increasing confinement strength. This is because the motion of the electrons is confined by the confining potential. With the increase of the confining potential ($\omega_{\parallel'}$ and $\omega_{z'}$, that is, with decreasing ρ' and z', the thermal motion energy of the electrons and the interaction between the electrons and phonons are enhanced because of the smaller particle motion range. As a result, the first internal excited state energy and the frequency of the transition spectral line of the polaron are all increased. These can also be attributed to the interesting quantum size effects.

From Eqs. (12) and (13), we can see that the relationships between the frequency of the transition spectral line of the strong-coupling polaron in a quantum rod varying with the electron–phonon coupling strength, the aspect ratio of the ellipsoid, the transverse radius of quantum rods and the transverse and longitudinal effective confinement length are all the same as the excitation energy.

In this paper only the interaction between the electron and the LO phonon is considered. When the size of the structure is small enough, the impact of the SO phonon on the polaron should also be included, which is neglected here for the sake of simplicity.

4. Conclusion

In conclusion, based on the linear combination operator method, we have investigated the first internal excited state energy, the excitation energy and the frequency of the transition spectral line of the strongly-coupled polaron in a quantum rod. It is found that the first internal excited state energy, the excitation energy and the frequency of the transition spectral line are increasing functions of the electron–phonon coupling strength, whereas they are decreasing ones of the transverse radius of quantum rods and the aspect ratio. The first internal excited state energy, the excitation energy and the frequency of the transition spectral line increase with decreasing transverse and longitudinal effective confinement length.

References

[1] Peng X, Manna L, Yang W, et al. Shape control of CdSe nanocrystals. Nature (London), 2000, 404: 59

[2] Kan S H, Mokari T, Rothenberg E, et al. Synthesis and size-dependent properties of zinc-blends semiconductor quantum rods.

Nature Mater, 2003, 2: 155

[3] Hu J T, Li L S, Yang W D, et al. Linearly polarized emission from colloidal semiconductor quantum rods. Science, 2001, 292: 2060

[4] Bruchez M, Moronne M, Gin P, et al. Semiconductor nanocrystals as fluorescent biological labels. Science, 1998, 281: 2013

[5] Chan W C W, Nie S. Quantum dot bioconjugates for ultrasensitive nonisotopic detection. Science, 1998, 281: 2016

[6] Klimov V I, Mikhailovsky A A, Xu S, et al. Optical gain and stimulated emission in nanocrystal quantum dots. Science, 2000, 290: 314

[7] Sek G, Podemski P, Misiewicz J, et al. Photoluminescence from a single InGaAs epitaxial quantum rod. Appl Phys Lett, 2008, 92: 021901

[8] Persano A, Leo G, Manna L, et al. Charge carrier transport in thin films of colloidal CdSe quantum rods. J Appl Phys, 2008, 104: 074306

[9] Bruhn B, Valenta J, Linnros J. Controlled fabrication of individual silicon quantum rods yielding high intensity, polarized light emission. Nanotechnology, 2009, 20: 505301

[10] Sreenivasan D, Haverkort J E M, Maksimenko S A, et al. Exciton radiative lifetime of quantum rods in reflectivity. Phys E, 2008, 40: 1985

[11] Creti A, Anni M, Rossi M Z, et al. Ultrafast carrier dynamics in core and core/shell CdSe quantum rods: role of the surface and interface defects. Phys Rev B, 2005, 72: 125346

[12] Creti A, Rossi M Z, Lanzani G, et al. Role of the shell thickness in stimulated emission and photoinduced absorption in CdSe core/shell nanorods. Phys Rev B, 2006, 73: 165410

[13] Zhang X W, Xia J B. Effects of shape and magnetic field on the optical properties of wurtzite quantum rods. Phys Rev B, 2005, 72: 205314

[14] Sun Z X, Swart I, Delerue C, et al. Orbital and charge-resolved polaron states in CdSe dots and rods probed by scanning tunneling spectroscopy. Phys Rev Lett, 2009, 102: 196401

[15] Katz D, Wizansky T, Millo O, et al. Size-dependent tunneling and optical spectroscopy of CdSe quantum rods. Phys Rev Lett, 2002, 89: 086801

[16] Li X Z, Xia J B. Electronic structure and optical properties of quantum rods. Phys Rev B, 2002, 66: 115316

[17] Li J B, Wang L W. High energy excitations in CdSe quantum rods. Nano Lett, 2003, 3: 101

[18] Zhang X W, Zhu Y H, Xia J B. Optical properties and g factors of GaAs quantum rods. Physica E, 2006, 33: 376

[19] Climente J I, Royo M, Movilla J L, et al. Strong configuration mixing due to dielectric confinement in semiconductor nanorods. Phys Rev B, 2009, 79: 161301(R)

[20] Talaat H, Abdallah T, Mohamed M B, et al. The sensitivity of the energy band gap to changes in the dimensions of the CdSe quantum rods at room temperature: STM and theoretical studies. Chem Phys Lett, 2009, 473: 288

[21] Wang C T, Xiao J L, Zhao C L. Ground-state energy of weak-coupling polarons in quantum rods. Journal of Semiconductors, 2009, 30(5): 072002

[22] Hu J T, Wang L W, Li S L, et al. Semiempirical pseudopotential calculation of electronic states of CdSe quantum rods. J Phys Chem B, 2002, 106: 2447

[23] Planelles J, Royo R, Ballester, et al. From quantum dots to quantum wires: electronic structure of semiconductor nanorods. Phys Rev B, 2009, 80: 045324

[24] Li S S, Xia J B. Spin-orbit splitting of a hydrogenic donor impurity in GaAs/GaAlAs quantum wells. Appl Phys Lett, 2008, 92: 022102